

AFRL TECHNICAL LIBRARY
KIRTLAND AFB, N.M.

TP
1644
c.1

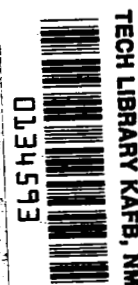
NASA Technical Paper 1644

**Effect of Oxide Additions and
Temperature on Sinterability
of Milled Silicon Nitride**

Alan Arias

APRIL 1980

NASA





NASA Technical Paper 1644

Effect of Oxide Additions and Temperature on Sinterability of Milled Silicon Nitride

Alan Arias
*Lewis Research Center
Cleveland, Ohio*



National Aeronautics
and Space Administration

**Scientific and Technical
Information Office**

1980



Summary

The purpose of the present investigation was to determine the sinterability of milled α - Si_3N_4 with oxide additions. MgO , CeO_2 , Y_2O_3 , and three mixtures involving two or more of these oxides were selected (from 10 oxides used in a preliminary evaluation) to determine the sinterability of α - Si_3N_4 with 0 to 5.07 equivalent percent oxide or oxide mixture additions. Batches usually containing one specimen of each composition were pressureless sintered for 4 hours in stagnant nitrogen at a fixed temperature in the 1650° to 1820° C range with the specimens covered with powdered Si_3N_4 + 5 weight percent SiO_2 . The resulting density-percent addition-temperature plots showed maxima which at most temperatures occurred between ~1.2 and 2.5 equivalent percent additive. The maximum densities obtained with each additive were as follows:

Additive		Sintering temperature, °C	Maximum density, percent of theoretical
Formula	Equivalent percent		
MgO	~1.24 to 1.87	1765 to 1820	98.5
CeO_2	2.5	1765 to 1820	99.6
Y_2O_3	2.5	1765 to 1820	99.2
Mixture of $\text{CeO}_2 + \text{Y}_2\text{O}_3$	~1.5 to 2.5	1820	98.6
Mixture of $\text{CeO}_2 + \text{MgO} + \text{Y}_2\text{O}_3$	1.24	1820	97.5
Mixture of $\text{CeO}_2 + \text{MgO} + \text{Y}_2\text{O}_3 + \text{ZrO}_2$	1.37	1820	98.5

Also, densities ≥ 94 percent of theoretical were obtained with as little as 0.62 equivalent percent additive (or, in wt. %: 1.0 MgO , 2.11 CeO_2 , etc.) on sintering at 1820° and, in some instances, at 1765° C.

X-ray diffraction showed that the materials were predominantly α - Si_3N_4 with some or no $\text{Si}_2\text{N}_2\text{O}$. Scanning electron photomicrographs showed microstructures of elongated grains with aspect ratios of about 5, for all additives.

Introduction

Silicon nitride (Si_3N_4) base ceramics have physical and chemical properties that make them prime candidates for applications in advanced heat engines and in other high temperature oxidizing environments. These ceramics are usually manufactured either by nitridation of silicon power compacts or by hot-pressing or pressureless sintering of Si_3N_4 powders. Partly because it allows near net-shape manufacturing of ceramics, pressureless sintering has received a great deal of attention in recent years despite the fact that this process also has some disadvantages. The main disadvantage of the pressureless sintering of Si_3N_4 is that the process requires sintering aids or additives (refs. 1 to 8) of the type and/or amounts that may be hazardous to health (such as BeN additions, ref. 8) or detrimental to the high temperature mechanical properties of the Si_3N_4 base ceramics (refs. 6, 7, and 9 to 11). It was surmised that low amounts of sintering aids may yield Si_3N_4 base ceramics with improved high temperature properties, provided these ceramics can be sintered to high densities. It was also surmised that the use of Si_3N_4 powders milled to a fine particle size might well provide the required sinterability with low amounts of additives, as was done in a previous investigation with Sialons (ref. 9 and 12).

The main objective of the present investigation was to determine the effects of various oxide additives and sintering temperatures on the sinterability of milled α - Si_3N_4 . To attain this objective, equivalent amounts of several oxides were separately mixed with milled α - Si_3N_4 , cold pressed, and sintered. The oxides showing the greatest effect on sinterability were then used either alone or in mixtures to determine the effects of sintering temperature and kind and amount of additive on sinterability. The sinterability and sintering behavior were determined by density measurements, weight and dimensional changes, optical and electron microscopy, and X-ray diffraction analyses of the sintered specimens.

Materials

The materials used in this investigation were α - Si_3N_4 and the 10 oxides listed in table I. These oxides were Al_2O_3 , CeO_2 , Cr_2O_3 , MgO , NiO , SiO_2 , Ta_2O_5 , Y_2O_3 , ZrO_2 , and Zyttrite ($\text{ZrO}_2 + 6.5$ mole % Y_2O_3). These materials were processed with equipment and by procedures described hereinafter.

Equipment

Two types of ball mills were used in this investigation: nickel-lined ball mills of 1500 cubic centimeter capacity with ~3700 grams of nickel shot (0.63 to 1.27 cm diam.), and type 430 stainless steel ball mills of 1500 cubic centimeter capacity with ~2500 grams of type 304 stainless steel balls (1.27 cm diam.). The rest of the equipment used in this investigation (presses, cold-pressing dies, furnaces, analytical equipment, etc.) was standard laboratory equipment.

Procedures

The procedures used for the preparation of the powders used for compounding the Si_3N_4 base ceramics are described briefly in table I and in more detail in the next section. The preparation of specimens from these powders is outlined in figure 1 and described in more detail in the following sections.

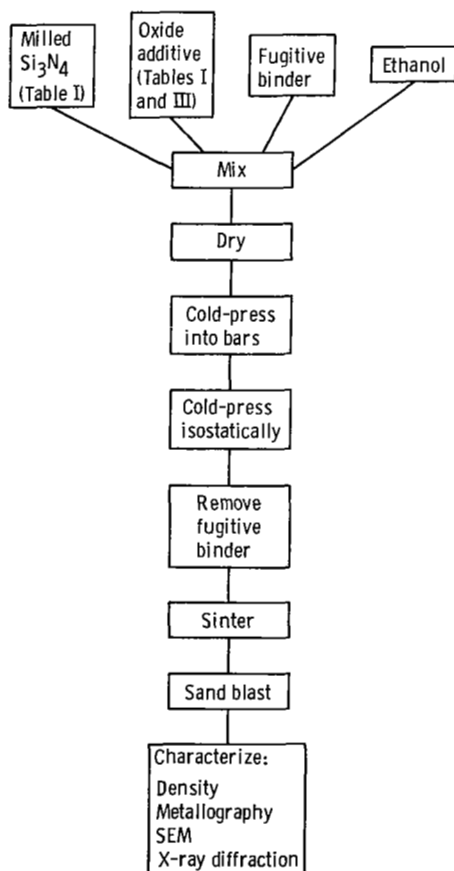


Figure 1. - Flow chart for the preparation and characterization of Si_3N_4 base ceramics.

Milling

The $\alpha\text{-Si}_3\text{N}_4$, SiO_2 , Cr_2O_3 , and ZrO_2 were separately milled with water as the milling fluid in the nickel-lined ball mills. The 200-gram batches of $\alpha\text{-Si}_3\text{N}_4$, Cr_2O_3 , and ZrO_2 were each milled for 300 hours. The 150-gram batch of SiO_2 was milled for 130 hours. As already pointed out in reference 13, during milling of the $\alpha\text{-Si}_3\text{N}_4$ there is a pressure buildup in the mill caused by hydrogen evolution resulting from the reaction of silicon (in the $\alpha\text{-Si}_3\text{N}_4$ used here) with water.

After drying them at 100°C , the unprocessed CeO_2 and Ta_2O_5 powders were separately dry milled in the stainless steel mills for 24 hours. The other oxide powders (Al_2O_3 , MgO , NiO , Y_2O_3 , and Zyt-trite) were not milled.

Removal of Pickup

During ball milling, materials resulting from wear of the balls and mills (pickup) contaminate the powders. The effects of the pickups on sinterability are unknown and for this reason they were removed whenever feasible. Most of the nickel pickup from the water-milled powders was removed magnetically, after separating the slurries from the nickel shot by sieving. The slurries were stirred while heating them, treated with 100 grams of reagent grade nitric acid, and then centrifuged to remove most of the liquid. The resulting moist powder was washed by stirring with heated distilled water. The wash water was then removed by centrifuging. The washing-centrifuging procedure was repeated twice more. The resulting powder cakes were vacuum dried at about 100°C and pulverized in a Waring blender. The dry powders were kept in air-tight containers until ready for use.

The dry-milled powders of CeO_2 and Ta_2O_5 were separated from the balls by sieving. No attempt was made to remove the (stainless steel) pickup from these oxides; in the case of CeO_2 , the pickup was relatively small (see analysis in table I). Besides, the CeO_2 could not be leached because it is soluble in most acids suitable for leaching out the stainless steel. In the case of Ta_2O_5 the pickup was larger (table I) but was not expected to affect the results significantly. After drying in air at about 100°C , these dry-milled powders as well as the five unprocessed oxides were then stored in air-tight containers until ready for use.

Chemical and BET Analyses

The powders listed in table I were analyzed for carbon and (spectrographically) for trace elements. The milled $\alpha\text{-Si}_3\text{N}_4$ was also analyzed for oxygen. The

specific surface areas of the powders were determined by the BET (Brunauer, Emmett, and Teller) method.

Mixing

The milled α - Si_3N_4 and the various oxides (table I) or mixtures of oxides (table II) additives making up the compositions investigated were weighed in an analytical balance. Each batch was placed in a polyethylene bottle with about twice its weight in type 304 stainless steel balls, 70 weight percent 200 proof ethanol, and 5 weight percent DC-705 silicon oil (as a temporary binder). Each batch of powder was mixed for 1 hour at 100 rpm. The resulting slurry was dried with constant stirring at about 100° C. After the balls were removed, the resulting power agglomerates were broken up in a Waring blender.

The amounts of oxide additives used in each batch are shown in tables III and IV. It may be noted in these tables that the amounts of the additives are stated both in weight and equivalent percent. The equivalent percent was calculated from the number of chemical equivalents of each component in the batches (additive, α - Si_3N_4 , and SiO_2 in the α - Si_3N_4). The number of chemical equivalents of a given compound (compound A, for example) is simply (weight of A)/(equivalent weight of A). Therefore, in a mixture of compounds A and B,

$$\text{equivalent \% of A} = \frac{\text{equiv. of A} \times 100}{\text{equiv. of A} + \text{equiv. of B}}$$

In the previous discussion, "equivalent weight" has the classical meaning, that is, the weight of an element or compound that reacts with, is produced from, or produces 1.008 grams of hydrogen. For calculation purposes, the normal valences of the elements (O^{-2} , N^{-3}) were used. It may be noted that the number of equivalents of a compound can also be obtained by multiplying the number of moles of this compound by the number of chemical bonds in the formula for the compound. Thus, for example, a hypothetical mixture of 7 moles of Si_3N_4 and 4 moles of SiO_2 would have $7 \times 4 \times 3 = 84$ equivalents of Si_3N_4 and $4 \times 2 \times 2 = 16$ equivalents of SiO_2 for a total of 100 equivalents. This mixture would then be 84 equivalent percent Si_3N_4 and 16 equivalent percent SiO_2 .

In the present investigation, batches of α - Si_3N_4 with the same equivalent percent of the various additives were used to facilitate comparisons of the effect of additives on sinterability.

Cold-pressing

The powder mixtures were shaped into bars approximately $3.18 \times 0.79 \times 0.39$ centimeters in a double acting steel die at a pressure of 207 megapascals (30 ksi). These bars were encased in plastic bags which were then evacuated, sealed, and isostatically cold-pressed at 483 megapascals (70 ksi).

Removing the Fugitive Binder

The silicone oil binder was removed from the cold-pressed bars by heating them in flowing nitrogen at 450° C for 1 hour.

Sintering

The bars to be sintered were measured and weighed. These bars were placed in a graphite boat and packed all around with a mixture of as received α - Si_3N_4 with 5 weight percent of as received SiO_2 (table I and ref. 12). A new batch of this powder pack was used for each run. Each sintering run at a given temperature normally included one bar of each composition investigated. All sintering runs were carried out in a furnace with graphite heating elements and under an atmosphere of stagnant nitrogen at 34.5 kilopascals (5 psi) gage pressure. The temperature range investigated was from 1650° to 1820° C and the time at temperature was 4 hours in all cases. The sintering temperatures were monitored and controlled with W/W-26 Re thermocouples. After sintering, the bars were sandblasted.

Characterization

The sintered and sandblasted bars were weighed and measured to determine weight loss and shrinkage. The density of these bars were determined either from their dimensions and weights or by water immersion depending on whether or not they were porous. Some of these bars were then either cut or broken into pieces suitable for optical microscopy, scanning electron microscopy (SEM), and X-ray diffraction analyses.

Hot-pressing

Mainly to compare densities, some of the compositions that showed good sinterability in preliminary experiments were also hot-pressed. Hot-pressing was done in a double acting graphite die at $1750 \pm 25^\circ$ C and 27.6 megapascals (4000 psi) for 30 minutes in flowing nitrogen. The resulting bars were assumed to be 100 percent dense. The as hot-pressed densities were then used to calculate the theoretical densities of

the pressureless sintered bars. It should be noted, however, that in preliminary experiments carried out prior to hot-pressing the theoretical densities used in the calculations were obtained based on the following assumptions:

(1) All the carbon in α - Si_3N_4 reacts with SiO_2 (on the α - Si_3N_4) to form SiO and CO (refs. 9 and 13).

(2) The remaining SiO_2 forms $\text{Si}_2\text{N}_2\text{O}$ (density = 2.85 g/cm^3).

(3) The oxide additives remained unchanged.

On the basis of the aforementioned assumptions, the fully dense α - Si_3N_4 of table I with no additives would have a density of 3.04 g/cm^3 .

Results and Discussion

Preliminary Evaluation of Sintering Aids

The oxides listed in table I were selected for evaluation as sintering aids mainly because of their relatively high melting points. Other oxides with relatively high melting points were not included in this preliminary evaluation for a variety of reasons. Some of them could have deleterious effects on high temperature mechanical properties (BaO , CaO , and SrO , ref. 10); others, such as BeO were considered to be hazardous to health; and still others had been previously tried by the author as sintering aids in unreported work and found either ineffective (TiO_2 , for example) or so hygroscopic (La_2O_3) that the cold-pressed compacts crumbled on standing in air.

To select the most promising aid for pressureless sintering, compositions of milled α - Si_3N_4 with each of the oxides listed in table I were prepared. In each of these compositions the amount of oxide additive used was equivalent to 4 weight percent of MgO , that is, all the compositions contained the same (~ 2.5) oxide equivalent percent. It should also be noted that the milled α - Si_3N_4 contains 7.72 weight percent oxygen which is equivalent to 14.5 weight percent SiO_2 . During sintering, this SiO_2 reacts with the 0.49 weight percent C in the milled α - Si_3N_4 (ref. 12), and the oxygen and SiO_2 are reduced to 6.60 and 12.41 weight percent, respectively.

Comparison of the as sintered densities listed in table III shows that the best sintering aids were Y_2O_3 , CeO_2 , MgO , Zyttrite, and Al_2O_3 all of which yielded sintered bars with better than 90 percent of theoretical density. These results agree, in part and qualitatively, with those of reference 14 where it was found that the best densifying agents for hot-pressed Si_3N_4 were CeO_2 , Ce_2O_3 , MgO , and La_2O_3 , and to a lesser extent Gd_2O_3 , Yb_2O_3 , BaO , and BeO . It is noteworthy that densities comparable to those obtained in reference 14 by hot-pressing were obtained by pressureless sintering in the present investigation with smaller amounts of MgO , CeO_2 ,

and Y_2O_3 . The densities of the best sintered materials from the present investigation (i.e., those with Y_2O_3 , CeO_2 , and MgO) are also greater than those of pressureless sintered Si_3N_4 with a variety of additives (including Y_2O_3 , CeO_2 , and MgO) reported in the literature (refs. 3 to 5 and 7).

Table III also shows that shrinkage was highest (8.9 to 12.8 percent) for the compositions that sintered to the highest densities. Except for the compositions containing MgO , relatively small (< 1.1 percent) weight losses occurred in the high density compositions. Regarding the relatively high weight loss (11.4 percent) of the composition containing MgO , it was noted that this composition (and others like it to be described later) formed a rather thick and relatively soft, whitish coating and a hard, dark gray core. The outer coating appears to be mostly β - Si_3N_4 and α -cristobalite, according to X-ray diffraction analysis.

Because of the encouraging results of this preliminary work, the investigation was extended to determine the effect of amounts of selected additives and sintering temperature on sinterability.

Effects of Type and Amounts of Additives and Sintering Temperatures on the Sinterability of Milled α - Si_3N_4

Additives used and temperature range investigated. — As shown in table III most of the 10 oxide additives used in the preliminary part of this investigation promoted densification. However, for the present more extensive part of the investigation, only the oxide additives from table III that yielded Si_3N_4 base ceramics with better than 95 percent of their theoretical density were further investigated. These oxides were MgO , CeO_2 , and Y_2O_3 . In addition, because of the relatively good results obtained with Zyttrite ($\text{ZrO}_2 + 6.5$ mole % Y_2O_3) as compared with ZrO_2 (table III) and also because of the apparent beneficial effects of oxide mixtures on sinterability reported in the literature (refs. 6 and 7), three oxide mixtures were also investigated as sintering aids for milled α - Si_3N_4 . These were a two-component ($\text{CeO}_2 + \text{Y}_2\text{O}_3$), a three-component ($\text{CeO}_2 + \text{Y}_2\text{O}_3 + \text{MgO}$), and a four-component ($\text{CeO}_2 + \text{Y}_2\text{O}_3 + \text{MgO} + \text{ZrO}_2$) mixture. The designations and oxide percent composition of these three mixtures are shown in table II.

In table IV are listed all the compositions used in this part of the investigation together with their designations, weight percent of additive, and equivalent percent of additive. It may be noted that each composition in table IV is designated by a letter (M for MgO , C for CeO_2 , Y for Y_2O_3 , etc.) and a numeral. In the case of compositions containing

MgO, this numeral is also the weight percent of MgO in the original mixture compounded from the materials in table I. For the other oxides the numeral in their designation does not correspond with their weight percent additive. However, all compositions having the same numeral in their designations contain the same equivalent percent of oxide additive. The equivalent percent shown in table IV was calculated on the assumption that the carbon in the materials reacted with SiO₂ to form and CO during sintering. As shown in table IV the amounts of additives used ranged from 0 to 5.071 equivalent percent.

Batches containing one bar from each of the compositions listed in table IV were sintered at 1700°, 1735°, 1765°, and 1820° C. In addition, one batch containing only one bar from each of the MgO compositions (M-0.5 to M-8, table IV) was sintered at 1650° C.

As shown in table III, two of the compositions sintered in the preliminary investigation had calculated theoretical densities greater than 100 percent, because of wrong assumptions regarding the composition and phases present in the pressureless sintered materials. To obviate this difficulty, the as hot-pressed densities were used as a basis of comparison in the present part of the investigation. For this comparison it was assumed that the hot-pressed and theoretical densities were the same.

Hot-pressed densities.—Figure 2 shows the densities of hot-pressed (HP) Si₃N₄ containing 0.617, 2.496, and 5.071 percent equivalent of each of the additives used in the present part of the investigation (MgO, CeO₂, Y₂O₃, and mixtures P, Q, and R, table IV). Compositions with mixtures Q and R were not actually hot-pressed; their values given in figure 2 were calculated from their theoretical densities and from the theoretical and the as hot-pressed densities of the corresponding compositions with mixture P. Thus, for example, at a given equivalent percent:

$$\text{HP dens. of Q} = \frac{\text{Theor. dens. of Q}}{\text{Theor. dens. of P}} \times \text{HP dens. of P}$$

wherein it was assumed that the ratio of the theoretical densities of compositions with P and Q mixtures equals the ratio of their as hot-pressed densities. As already stated in the PROCEDURES section, the density of fully dense, milled Si₃N₄ without additives was calculated to be 3.04 g/cm³ and this is the value plotted in figure 3 at 0 percent additive. As figure 2 shows, the densities of the hot-pressed compositions extrapolate quite well to 0 percent additive.

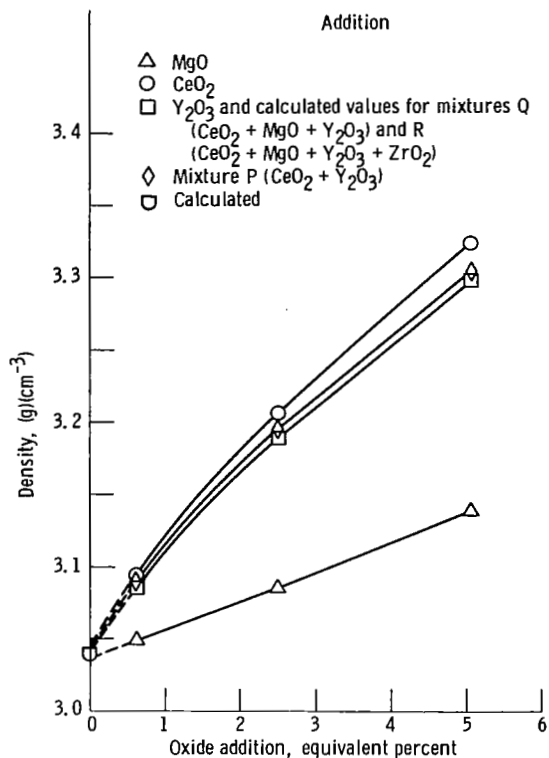


Figure 2. - Densities of hot-pressed Si₃N₄ with oxide additions.

Effect of Composition and Sintering

Temperature on Density

Effect of single oxide additions.—Figure 3 shows the effect of MgO additions and sintering temperature on the density of pressureless sintered Si₃N₄. At all sintering temperatures, the density increases steeply with increasing MgO additions near the origin of the plots. As a rule, the higher the sintering temperature the steeper this density increase, except perhaps for the 1650° C plot whose density near the origin is unknown, because the data point for 0 percent MgO is missing. After the initial steep increase in density, the steepness of the plots gradually decreases, the density reaches a maximum between about 0.93 and 1.87 equivalent percent (1.5 to 3 wt.%) MgO, then the density decreases with increasing MgO. In most cases, this decrease in density with MgO in excess of about 1.87 equivalent percent was accompanied by bloating. Maximum densities of about 98.5 percent of theoretical were obtained by sintering compositions with 1.24 to 1.87 equivalent percent (2 to 3 wt.%) MgO. As a rule, the higher the sintering temperature the lower the amount of MgO

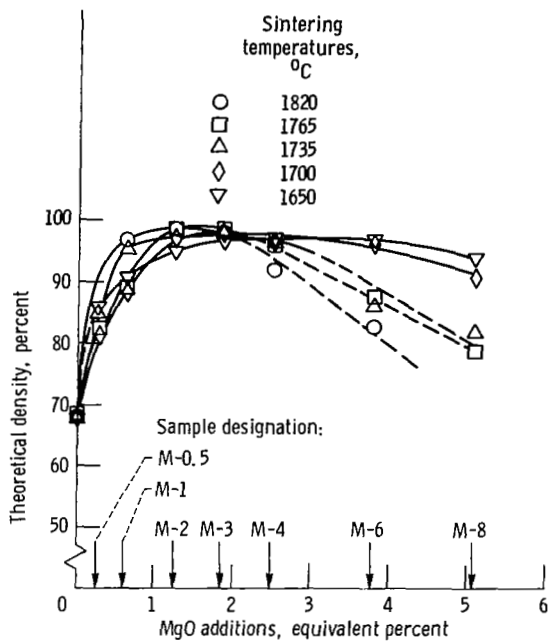


Figure 3. - Effect of MgO additions and sintering temperature on density of pressureless sintered Si_3N_4 . (All samples sintered for 4 hr in N_2 .)

at which maximum density occurred. As the plots indicate, it is possible to obtain materials with 96 percent or better of their theoretical densities by sintering at high temperatures (1765° to 1820° C) with as little as 0.62 equivalent percent (1 wt.%) MgO. These are the highest densities so far reported in the literature for pressureless sintered Si_3N_4 with such small amounts of additive. Sintering at lower temperatures (1650° C) with 1.55 to 4.42 equivalent percent (2.5 to 7 wt.%) MgO also gave densities in excess of 96 percent of theoretical.

Figure 4 shows the effects of CeO_2 additions and sintering temperature on the density of pressureless sintered Si_3N_4 . Here again the density increases with increasing additive, reaches a maximum, and then declines. In this case, however, the maxima all occur at about 2.5 equivalent percent (8.17 wt.%) CeO_2 . Beyond this value all compositions sinter about equally well at all the temperatures investigated, but the density decreases with increasing CeO_2 . As the plots show it is possible to sinter these compositions to 95 percent of theoretical density with as little as 0.62 equivalent percent (2.11 wt.%) of CeO_2 . In this system, the maximum density was 99.6 percent of theoretical and was obtained at 2.5 equivalent percent (8.17 wt.%) and 1765° to 1820° C.

Figure 5 shows the effect of Y_2O_3 additions and sintering temperatures on the density of pressureless sintered Si_3N_4 . Here again, the plots show maxima

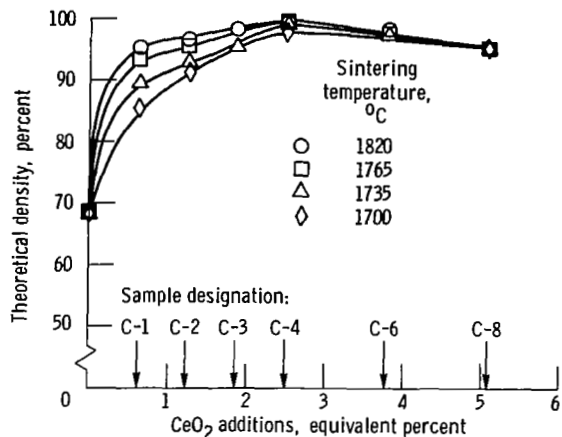


Figure 4. - Effect of CeO_2 additions and sintering temperature on density of pressureless sintered Si_3N_4 . (All samples sintered 4 hr in N_2 .)

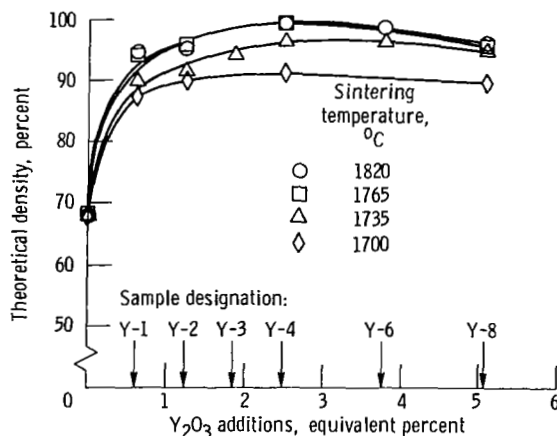


Figure 5. - Effect of Y_2O_3 additions and sintering temperature on density of pressureless sintered Si_3N_4 . (All samples sintered 4 hr in N_2 .)

at about 2.5 equivalent percent (7.22 wt.%). For this system the maximum density obtained was 99.2 percent of theoretical at 2.5 equivalent percent and 1765° to 1820° C. In general, in the lower temperature range ($\leq 1735^\circ$ C) compositions containing Y_2O_3 did not sinter as well as those with CeO_2 or MgO. However, in the high temperature sintering range ($\geq 1735^\circ$ C) it was possible to obtain densities ≥ 94 percent of theoretical with as little as 0.62 equivalent percent (1.85 wt.%) Y_2O_3 .

From the aforementioned, it may be concluded that the maximum densities obtainable on sintering with MgO, CeO_2 , or Y_2O_3 additives are about the same, within the limits of experimental error. However, either on a weight percent or an equivalent percent basis, MgO is a more effective sintering aid than either CeO_2 or Y_2O_3 . On an equivalent percent

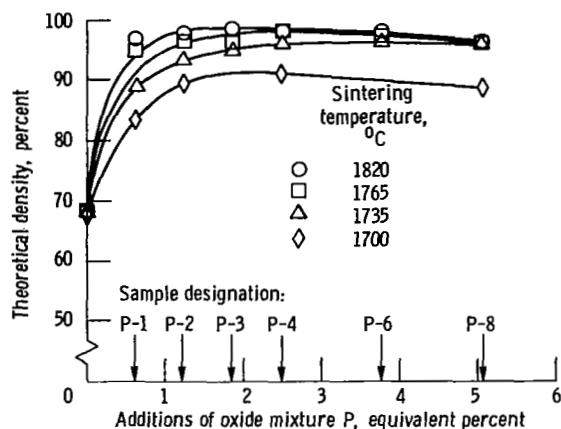


Figure 6. - Effect of additions of oxide mixture P ($\text{CeO}_2 + \text{Y}_2\text{O}_3$) and sintering temperature on density of pressureless sintered Si_3N_4 . (All samples sintered 4 hr in N_2 .)

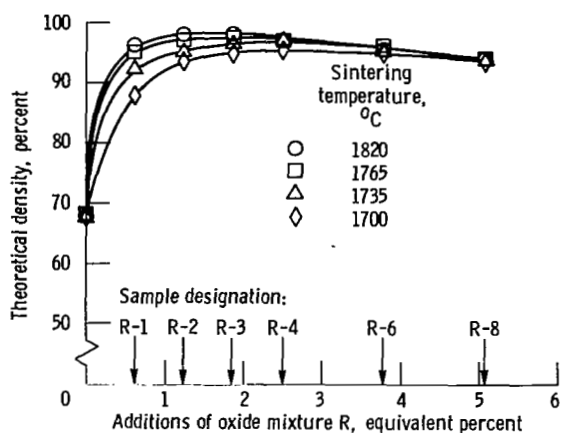


Figure 8. - Effect of additions of oxide mixture R ($\text{CeO}_2 + \text{Y}_2\text{O}_3 + \text{MgO} + \text{ZrO}_2$) and sintering temperature on density of pressureless sintered Si_3N_4 . (All samples sintered 4 hr in N_2 .)

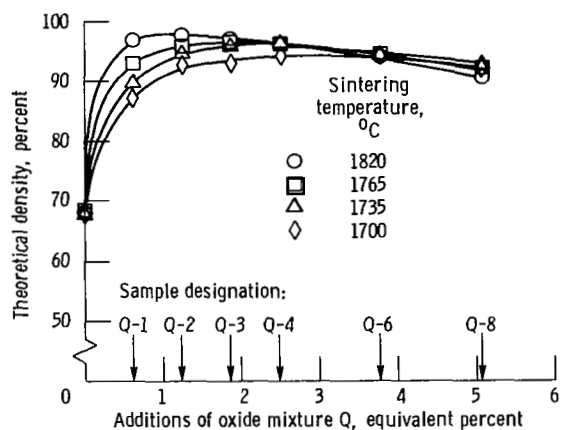


Figure 7. - Effects of additions of oxide mixture Q ($\text{CeO}_2 + \text{Y}_2\text{O}_3 + \text{MgO}$) and sintering temperature on density of pressureless sintered Si_3N_4 . (All samples sintered 4 hr in N_2 .)

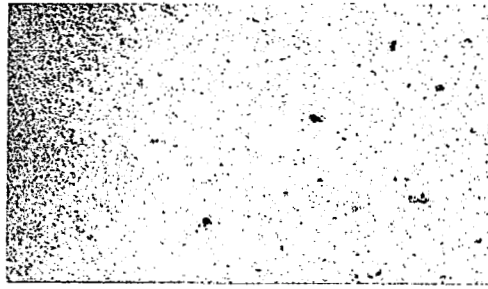
basis, CeO_2 and Y_2O_3 are about equally effective as sintering aids, except that CeO_2 appears to be somewhat more effective than Y_2O_3 at temperatures below about 1735°C .

Effect of oxide mixture additions. - Figures 6, 7, and 8 show the effects of additions of mixtures P, Q, and R, respectively, and sintering temperature on the density of pressureless sintered Si_3N_4 . The maximum densities obtained were 98.6 percent of theoretical for compositions with mixture P (at ~1.5 to 2.5 equivalent % and 1820°C , fig. 6); 97.5 percent of theoretical for compositions with mixture Q (at 1.24 equivalent % and 1820°C , fig. 7); and 98.5

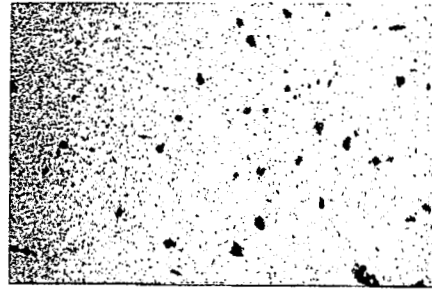
percent of theoretical for compositions with mixture R (at 1.87 equivalent % and 1820°C , fig. 8). The plots obtained with the three oxide mixtures are very similar in shape to those obtained with single oxide additives. Thus, the densities increase rapidly with composition at low values of equivalent percent, all plots show density-composition maxima, and in most cases the density decreases slightly with increasing composition at addition levels greater than about 2.5 equivalent percent. In other words, as with single oxides, in most cases the density changes with composition are relatively insensitive to composition at >2.5 equivalent percent addition.

In general, the plots obtained with oxide mixtures reflect the combined effects of the separate oxide additives. Thus, for instance, the Y_2O_3 in composition with mixture P (fig. 6) decreases sinterability in the low temperature ($<1735^\circ\text{C}$) sintering range and the MgO in compositions with mixtures Q and R (figs. 7 and 8) causes the density maxima to shift down to about 1.2 equivalent percent additive. As with MgO and CeO_2 densities ≥ 95 percent of theoretical can be obtained with as little as 0.62 equivalent percent of any of the three mixtures. Also, in the plots for either single oxides or oxide mixture additives the increases in density with amount of additive (i.e., the slopes of the density-equivalent % plots) are largest near the origin. This indicates that, other things being equal, small amounts of suitable additives or impurities can have a relatively large effect on the sinterability of Si_3N_4 .

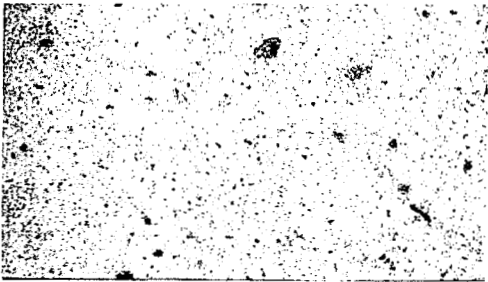
Shrinkage and weight losses on pressureless sintering. - Table V lists representative linear (length) shrinkages and weight losses of compositions involving additions of the three single oxides and the three mixtures at all the temperatures investigated. As



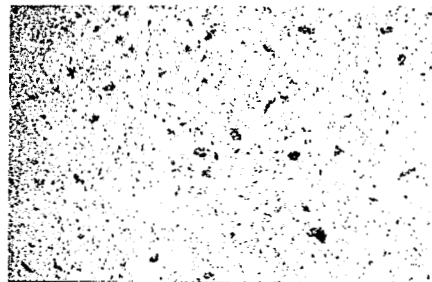
(a) MgO = 1.24 equivalent % (M-2). Density = 3.02 g/cm³. Sintered at 1765° C.



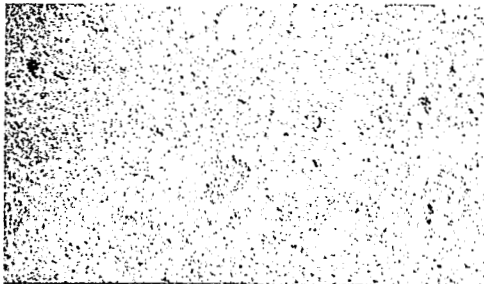
(b) CeO₂ = 2.5 equivalent % (C-4). Density = 3.20 g/cm³. Sintered at 1765° C.



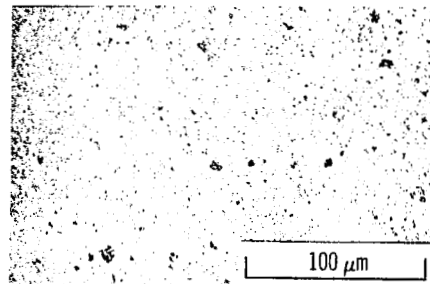
(c) Y₂O₃ = 2.5 equivalent % (Y-4). Density = 3.16 g/cm³. Sintered at 1765° C.



(d) P mixture = 2.5 equivalent % (P-4). Density = 3.14 g/cm³. Sintered at 1765° C.



(e) Q mixture = 1.24 equivalent % (Q-2). Density = 3.05 g/cm³. Sintered at 1820° C.



(f) R mixture = 1.87 equivalent % (R-3). Density = 3.11 g/cm³. Sintered at 1820° C.

Figure 9. - Light photomicrographs of Si₃N₄ base compositions with the highest densities. All compositions were pressureless sintered 4 hours in stagnant nitrogen at temperature indicated under each photomicrograph. Unetched.

shown in the table, shrinkages varied from 8.5 to 13.1 but the best sintered specimens (density >98 percent of theoretical) showed shrinkages from about 12 to 13.1 percent. However, shrinkage alone is not a good criteria for determining sinterability mainly because shrinkage involves the combined effects of sintering and weight losses.

In general, weight losses increase with increasing sintering temperature. This was to be expected, in view of the well known fact that Si₃N₄ both decomposes and reacts with SiO₂ at high temperature (refs. 12 and 13). However, considering both decomposition and reaction, most of the compositions show

surprisingly small weight losses even after sintering at 1820° C. Thus, except for MgO-bearing compositions (to be discussed in the next paragraph) most of the other compositions in table V with ~2.5 equivalent percent additive (C-4, Y-4, P-4, Q-4, and R-4) had weight losses ≤2.6 percent and sintered to better than 97 percent of theoretical density at 1820° C. The small extent of these weight losses is attributed to the beneficial effects of the sintering powder pack cover used (ref. 12).

It is readily apparent from the data in table V that the largest weight losses occurred in compositions containing only MgO as the additive. These MgO-



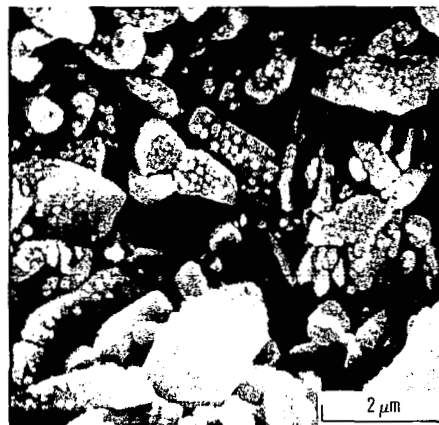
(a) MgO additive (M-4).



(b) CeO₂ additive (C-4).



(c) Y₂O₃ additive (Y-4).



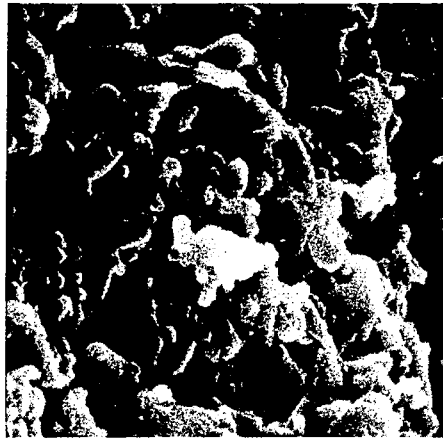
(d) Mixture P additive = CeO₂ + Y₂O₃ (P-4).

Figure 10. - Scanning electron micrographs of fracture surfaces of Si₃N₄ base compositions with 2.5 equivalent percent of additives indicated after pressureless sintering at 1765° C for 4 hours. Etched.

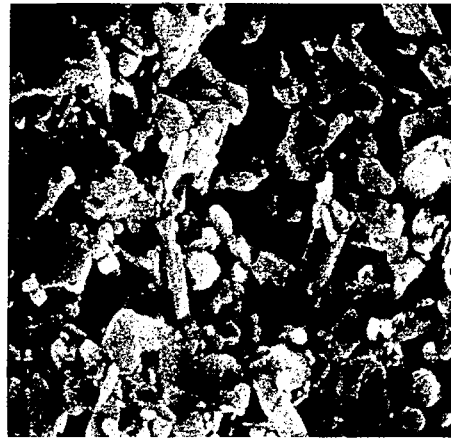
containing compositions with high weight losses usually consisted of a dark, hard core and a light colored coating abrasible by sandblasting. However, as shown in the plots in figure 3 and the data in table V, it was possible to obtain reasonably well sintered (~97 percent theoretical density) MgO-bearing compositions with very small weight losses by sintering at 1650° C.

Microstructures. - In figure 9 are shown light photomicrographs of compositions made with the six different additives used in this part of the investiga-

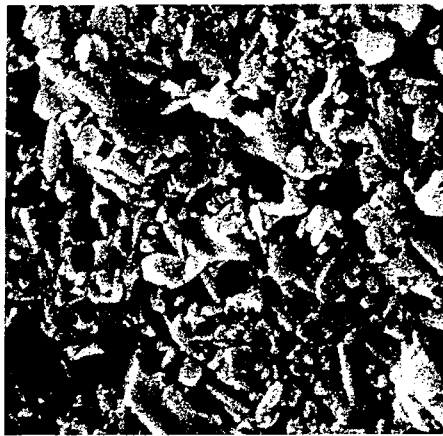
tion and having the best obtainable densities for each kind of additive. All six photomicrographs show well sintered, relatively pore-free materials. The matrices of all six materials are two-phase. Small amounts of a rounded, dark gray phase are embedded in the matrices, and still smaller amounts of bright, metallic-looking specks of a fourth phase are also embedded in the matrices. The same four phases (two matrix phases, a dark gray phase, and metallic-looking specks) appear in all the compositions and at all the temperatures investigated. As a rule, the larger



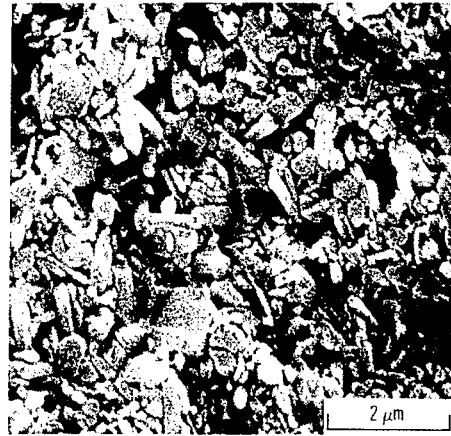
(a) 0.308 equivalent % MgO (M-0.5).



(b) 1.24 equivalent % MgO (M-2).



(c) 2.5 equivalent % MgO (M-4).



(d) 5.07 equivalent % MgO (M-8).

Figure 11. - Scanning electron photomicrographs of Si_3N_4 with MgO additions after pressureless sintering at 1650°C for 4 hours in stagnant nitrogen. Etched.

the amount of additive and the higher the sintering temperature the larger the amount of the dark gray phase. The metallic-looking specks are probably silicon or a silicon base alloy (ref. 12). For reasons to be discussed in the next section, it is surmised that the matrix phases are $\alpha\text{-Si}_3\text{N}_4$ and $\text{Si}_2\text{N}_2\text{O}$ and that the dark gray phase is probably glass.

Figure 10 shows scanning electron photomicrographs of four of the compositions after sintering at 1765°C . Although not shown, the microstructures of compositions made with mixtures Q and R were very similar. The specimens shown in figure 10 were all etched in fused 40 KOH:40 NaOH:20 LiOH at 180°C for 30 minutes (ref. 8). All of these etched samples have elongated grains with an aspect ratio of about 5 and average length of about 2 micrometers. The grain shape and size appears to be fairly independent of the kind and amount of additive, as seen in figure 10 for four different kinds of

additives, and in figure 11 for different amounts of the same MgO additive. Grain size, however, increases with increasing sintering temperature, as evidenced by comparison of figures 11(c) (M-4, 1650°C) and 10(a) (M-4, 1765°C). The elongated grain structure was developed during sintering, since, as shown in the scanning electron photomicrograph of figure 12, the milled $\alpha\text{-Si}_3\text{N}_4$ powder is very fine and equiaxed. The uniform wart-like deposits on the grains in figure 10(d) are probably artifacts formed during metallographic preparation.

The transformation of equiaxed α to elongated $\beta\text{-Si}_3\text{N}_4$ grains that occurred during pressureless sintering, as found in the present investigation and by others (refs. 5 and 8), may lead to Si_3N_4 base ceramics with improved bend strength and fracture toughness (ref. 15).

X-ray diffraction analyses and implications. - From the chemical composition of

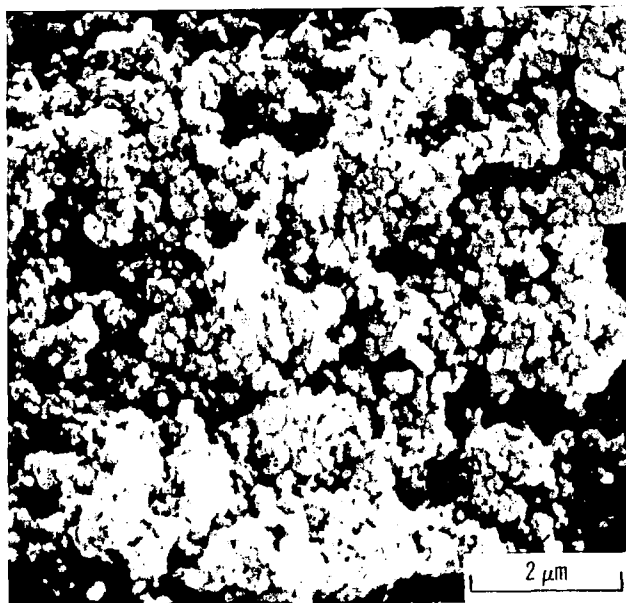


Figure 12. - Scanning electron photomicrograph of fracture surface of as cold pressed Si_3N_4 without additives.

the starting mixtures (table IV) it is possible to determine the equilibrium phases that should be present in the various sintered compositions, provided the corresponding equilibrium phase diagrams are available. Thus, for instance, all the compositions investigated with MgO as a single addition fall within the Si_3N_4 - Mg_2SiO_4 - $\text{Si}_2\text{N}_2\text{O}$ compatibility triangle of the Si_3N_4 -MgO- SiO_2 system (ref. 16), and all the compositions investigated with Y_2O_3 as a single addition fall within the Si_3N_4 - $\text{Y}_2\text{Si}_2\text{O}_7$ - $\text{Si}_2\text{N}_2\text{O}$ compatibility triangle of the Si_3N_4 - Y_2O_3 - SiO_2 system (ref. 17). It is surmised that the compositions containing single additions of CeO_2 should probably be also three-phase but the Si_3N_4 - CeO_2 - SiO_2 phase diagram could not be found in the literature. Therefore, in view of the aforementioned phase relationships, it was interesting to see that, as shown by the X-ray diffraction analyses in table VI, the compositions from the present investigation were predominantly β - Si_3N_4 with small amounts of $\text{Si}_2\text{N}_2\text{O}$. The tridymite or α -cristobalite detected in some of the samples was probably on the sandblasted surfaces surrounding the ground surfaces on which the analyses were taken. Thus, despite the fact that some of the compositions (M-8, C-8, and Y-8, for example) have relatively large amounts of additives these were not detected (as compounds such as Mg_2SiO_4 , $\text{Y}_2\text{Si}_2\text{O}_7$, etc.) by X-ray diffraction. Yet these additives must have been largely retained in the sintered materials because in most cases the percent weight losses during sintering (table V) were smaller than the

weight percent of additive used. It may also be noted that compositions with large amounts of a single additive (such as M-8, C-8, and Y-8) and sintered at high temperature show either β - Si_3N_4 alone or β - Si_3N_4 with very small amounts of $\text{Si}_2\text{N}_2\text{O}$. Within the limits of experimental error the lattice parameters of these two phases appear to be constant and independent of the amount of additive. From these facts it is concluded that the additives are probably mostly in a glass phase (undetected by X-ray diffraction) and that the amount of this nitrogen-rich glass phase probably increases with the amount of additive and with sintering temperature. These views are further supported by the fact that the amount of the gray phase seen in light photomicrographs increases with increasing amounts of additive. It follows from the previous discussion that the two matrix phases seen in all the optical photomicrographs (fig. 9) are β - Si_3N_4 and (probably) $\text{Si}_2\text{N}_2\text{O}$ and that the rounded, dark gray phase is probably a glass.

Summary of Results and Conclusions

The present investigation was conducted to determine the effects of oxide additions and sintering temperatures on the sinterability of milled α - Si_3N_4 . Cold-pressed powder compacts were pressureless sintered in the 1650° to 1820° C temperature range for 4 hours in stagnant nitrogen with the compacts covered with a powdered mixture of coarse Si_3N_4 + 5 weight percent SiO_2 . The result obtained and some of the conclusions drawn therefrom can be summarized as follows:

1. On sintering Si_3N_4 containing from 0 to 5.071 equivalent percent of MgO, CeO_2 , or Y_2O_3 or with binary, ternary, or (with ZrO_2) quaternary mixtures of these oxides it was found that the density-composition plots showed density maxima whose location in the plot depended on the type and amount of additive and on sintering temperature. Optimum results were as follows:

a. On sintering Si_3N_4 with MgO additions at 1765° to 1820° C a maximum density of about 98.5 percent of theoretical was obtained in the range of ~1.24 to 1.87 equivalent percent (~2 to 3 wt.%) MgO.

b. On sintering Si_3N_4 with CeO_2 additions at 1765° to 1820° C a maximum density of 99.6 percent of theoretical was obtained with 2.5 equivalent percent (8.17 wt.%) CeO_2 .

c. On sintering Si_3N_4 with Y_2O_3 additions at 1765° to 1820° C a maximum density of 99.2 percent of theoretical was obtained with 2.5 equivalent percent (7.22 wt.%) Y_2O_3 .

d. On sintering Si_3N_4 with additions of a binary mixture of CeO_2 and Y_2O_3 at 1820° C a maximum density of 98.6 percent of theoretical

was obtained with ~1.5 to 2.5 equivalent percent (~4.72 to 7.69 wt. %) of the mixture.

e. On sintering Si_3N_4 with additions of a ternary mixture of MgO , CeO_2 , and Y_2O_3 at 1820°C a maximum density of 98.6 percent of theoretical was obtained with 1.24 equivalent percent (3.29 wt. %) of the mixture.

f. On sintering Si_3N_4 with additions of a quaternary mixture of MgO , CeO_2 , Y_2O_3 , and ZrO_2 at 1820°C , a maximum density of 98.5 percent of theoretical was obtained with 1.87 equivalent percent (4.80 wt. %) of the mixture.

2. Sintered densities ≥ 94 percent of theoretical were obtained with all six additives at 1820°C and with as little as 0.62 equivalent percent of additive.

3. The density-composition plots for all six additives show a rapid increase in density with composition at the origin of the plots. From this it is concluded that small amounts of suitable additives or impurities can have a relatively large effect on sinterability.

4. X-ray diffraction and light microscopy analyses of sintered samples indicate that regardless of type and amount of additive, the compositions investigated are made up mainly of $\beta\text{-Si}_3\text{N}_4$ with small amounts of $\text{Si}_2\text{N}_2\text{O}$ and (probably) a glass.

5. Scanning electron photomicrographs show that the originally equiaxed powder was converted during sintering to elongated grains having aspect ratios of about 5. The grain size did not appear to be significantly dependent on composition but it increased with sintering temperature. This type of microstructure may lead to Si_3N_4 base ceramics of improved strength and fracture toughness.

Lewis Research Center,
National Aeronautics and Space Administration,
Cleveland, Ohio, December 4, 1979,
505-01.

References

1. Jack, K.H.; and Wilson, W.I.: *Ceramics Based on the Si-Al-O-N and Related Systems*. Nature (London), Phys. Sci., vol. 238, no. 80, 1972, pp. 28-29.
2. Wills, R.R.: Reaction of Si_3N_4 with Al_2O_3 and Y_2O_3 . J. Am. Ceram. Soc., vol. 58, no. 7-8, 1975, p. 335.
3. Terwilliger, G.R.; and Lange, F.F.: Pressureless Sintering of Si_3N_4 . J. Mat. Sci., vol. 10, July 1975, pp. 1169-1174.
4. Mitomo, M.; et al.: Sintering of Si_3N_4 . Am. Ceram. Soc. Bull., vol. 55, no. 3, Mar. 1976, p. 313.
5. Oda, I.; Kaneno, M.; and Yamamoto, N.: Pressureless Sintered Silicon Nitride, Nitrogen Ceramics, Riley, F.L., ed., Noordhoff, (Leyden), 1977, pp. 359-365.
6. Rae, A.W.J.M.; Thompson, D.P.; and Jack, K.H.: The Role of Additives in the Densification of Nitrogen Ceramics. Ceramics for High Performance Applications-II, Burke, J.J.; Leno, E.N.; and Katz, R.N., eds., Brook Hill Publishing Co., Mass., 1978, pp. 1039-1067.
7. Smith, J.T.: GTE Si_3N_4 -Based Ceramics. Highway Vehicles Systems Contractor's Coordination Meeting, 16th., CONF-7904105, U.S. Dept. of Energy, 1979, pp. 171-179.
8. Prochazka, S.; and Greskovich, C.D.: Development of a Sintering Process for High-Performance Silicon Nitride. SRD-77-178, General Electric Co., 1978. (AMMRC-TR-78-32, AD-A061880.)
9. Arias, A.: Pressureless Sintered Sialons with Low Amounts of Sintering Aid. NASA TP-1246, 1978.
10. Iskoe, J.L.; Lange, F.F.; and Diaz, E.S.: Effect of Selected Impurities on the High Temperature Mechanical Properties of Hot-Pressed Silicon Nitride. J. Mater. Sci., vol. 11, May 1976, pp. 908-912.
11. Weaver, G.Q.; and Lucek, J.W.: Optimization of Hot-Pressed $\text{Si}_3\text{N}_4\text{-Y}_2\text{O}_3$ Materials. Am. Ceram. Soc. Bull., vol. 57, no. 12, Dec. 1978, pp. 1131-1134 and 1136.
12. Arias, A.: Effect of Oxygen-Nitrogen Ratio Sinterability of Sialons. NASA TP-1382, 1979.
13. Jack, K.H.: Sialons and Related Nitrogen Ceramics. J. Mater. Sci., vol. 11, June 1976, pp. 1135-1158.
14. Huseby, I.C.; and Petzow, G.: Influence of Various Densifying Additives on Hot-Pressed Si_3N_4 . Powder Metall. Int., vol. 6, no. 1, 1974, pp. 17-19.
15. Himsolt, G., et al.: Mechanical Properties of Hot-pressed Silicon Nitride with Different Grain Structures. J. Am. Ceram. Soc., vol. 62, no. 1-2, Jan.-Feb. 1979, pp. 29-32.
16. Lange, F.F.: Phase Relations in the System $\text{Si}_3\text{N}_4\text{-SiO}_2\text{-MgO}$ and Their Interrelation with Strength and Oxidation. J. Am. Ceram. Soc., vol. 61, no. 1-2, Jan.-Feb. 1978, pp. 53-56.
17. Lange, F.F.; Singhal, S.C.; and Kuznicki, R.C.: Phase Relations and Stability Studies in the $\text{Si}_3\text{N}_4\text{-SiO}_2\text{-Y}_2\text{O}_3$ Pseudoternary System. J. Am. Ceram. Soc., vol. 60, no. 5-6, May-June 1977, pp. 249-252.

TABLE I. - MATERIALS CHARACTERIZATION

Material	Source and designation	Milling data				Post-milling treatment	Specific surface area of milled powder, m ² /g	Chemical analysis ^a		
		Mill material	Balls	Milling fluid	Milling time, hr			Oxygen, percent	Carbon, percent	Other elements, ppm unless noted otherwise (spectrographic analyses)
α -Si ₃ N ₄	Kawecki-Berylco Industries, CP-85	Ni	Ni	Water	300	Leach, centrifuge, wash, centrifuge, dry	22.9	7.72	0.20 ^b 0.49	0.4% Al-540 Ca-200 Cr-30 Cu-0.1% Fe-80 Mg-70 Mn-180 Mo-240 Ni-230 Ti-140 Zr-Si major
Al ₂ O ₃	Union Carbide Corp., Linde A	-----	-----	-----	0	-----	14.5	(c)	0.019	80 Ca-<10 Co-5Cr-<50 Cu-20 Fe-<5 Mn-<20 Mo-<100 Nb-<5 Ni-50 Pb-50 Sn-20 Ti-<10 V-<40 W-<100 Y-<10 Zr
CeO ₂	Cerac Pure, C-1064	Stainless steel	Stainless steel	Air	24	None	35.4	(c)	0.019	340 Ca-0.2% Cr-0.3% Fe-250 Mg-630 Mo-450 Ni-Ce major
Cr ₂ O ₃	Fisher Scientific, C-334	Ni	Ni	Water	300	Same as α -Si ₃ N ₄ above	20.3	(c)	0.023	640 Al-90 Ca-40 Cu-490 Fe-0.4% Ni-620 V-Cr major
MgO	Fisher Scientific, M-300	-----	-----	-----	0	-----	19.6	(c)	0.675	130 Al-0.2% Ca-200 Fe-Mg major-120 Mn-840 Si-80 Ti
NiO	Fisher Scientific, N-69	-----	-----	-----	0	-----	2.55	(c)	0.005	50 Cr-70 Cu-60 Fe-30 Mg-20 Mn-Ni major-<10 Si
SiO ₂	Cerac Pure, S-1061	Ni	Ni	Water	300	Same as α -Si ₃ N ₄ above	27.1	(c)	0.037	630 Al-130 Ca-70 Cr-110 Cu-80 Fe-210 Mg-Si major-900 Ni
Ta ₂ O ₅	Cerac Pure, T-1013	Stainless steel	Stainless steel	Air	24	None	1.7	(c)	0.005	0.2% Al-310 Ca-160 Co-1.5% Cr-120 Cu-2.8% Fe-70 Mg-850 Mn 0.3% Si-Ta major-860 Zr
Y ₂ O ₃	Research Chemicals, 99.9% pure	-----	-----	-----	0	-----	69.9	(c)	0.144	50 Al-75 Ca-<10 Co-2 Cr-<50 Cu-<20 Fe-<5 Mn-<20 Mo-2000 Na-<100 Nb-5 Ni-<100 Pb-<50 Sn-5 Ti-<10 V-<40 W-Y major-<10 Zr
ZrO ₂	Zirconium Corp. of America, Grade AH	Ni	Ni	Water	300	Same as α -Si ₃ N ₄	35.5	(c)	0.063	120 Al-410 Ca-60 Cr-80 Cu-430 Fe-0.9% Ni-0.4% Si-120 Ti-Zr major
Zyttrite	HTM Co., Zyttrite-6.5	-----	-----	-----	0	-----	(d)	(c)	0.22	ZrO ₂ stabilized with 6.5 mole % Y ₂ O ₃ ; impurities not including Hf < 300 ppm (manufacturer's data)

^aAnalysis of materials used for compounding batches.

^bThis carbon content obtained after mixing 1 hr with 5 wt. % silicone oil and 70 wt. % ethanol then heating at 450° C for 1 hr in flowing nitrogen.

^cNot determined.

^dAverage particle size <100 Å (manufacturer's data).

TABLE II. - COMPOSITION OF OXIDE MIXTURES
USED AS ADDITIVES

Mixture designation	Composition		
	Oxides in mixture ^a	Mole percent oxide	Weight percent oxide
P	CeO ₂	60	53.34
	Y ₂ O ₃	40	46.66
Q	CeO ₂	27.27	42.68
	MgO	54.55	19.99
	Y ₂ O ₃	18.18	37.33
R	CeO ₂	21.43	32.69
	MgO	42.85	15.31
	Y ₂ O ₃	14.29	28.60
	ZrO ₂	21.43	23.40

^aThe pure oxides used are described in table I.

TABLE III. - RESULTS OF PRELIMINARY SINTERING EXPERIMENTS: DENSITY, SHRINKAGE, AND WEIGHT LOSS OF Si_3N_4 BASE CERAMICS CONTAINING OXIDE ADDITIVES AFTER SINTERING AT 1765°C FOR 4 HOURS IN STAGNANT NITROGEN

Oxide addition (table I)		Green density of compacted mixture, g/cm^3 ^b	Sintered materials				
Formula	Weight percent ^a		Calculated, theoretical density, g/cm^3 ^c	As sintered density		Shrinkage,	Weight loss, percent
				g/cm^3	Percent of theoretical		
Al_2O_3	3.335	1.97	3.06	^d ~2.76	^d ~90.2	^d ~8.9	0.9
CeO_2	8.167	2.08	3.19	3.20	100.3	12.8	1.1
Cr_2O_3	4.975	1.99	3.10	2.10	67.7	4.6	9.8
MgO	4.000	1.97	3.06	2.92	95.4	12.3	11.4
NiO	7.166	2.04	3.17	2.13	67.2	3.5	10.4
SiO_2	3.011	1.94	3.01	2.01	66.8	6.3	14.8
Ta_2O_5	8.366	2.09	3.22	^d ~2.19	^d ~68.0	^d ~4.8	9.6
Y_2O_3	7.217	2.00	3.13	3.16	101.0	12.4	-0.1
ZrO_2	5.986	1.99	3.14	2.50	79.6	8.5	5.3
Zyttrite	6.060	2.00	3.14	2.91	92.7	10.7	1.0

^aAll compositions contain 2.496 equivalent percent of oxide addition.

^bAfter isostatic cold pressing and removal of the temporary binder at 450°C (see text).

^cCarbon in Si_3N_4 (0.49 wt. %) assumed to react with SiO_2 to form volatile SiO and CO . The rest of the SiO_2 assumed to form $\text{Si}_2\text{N}_2\text{O}$. Additives (other than SiO_2) assumed to remain unchanged.

^dApproximate sign (~) indicates that the sintered specimen was either bent or chipped.

TABLE IV. - ADDITIVES, COMPOSITIONS INVESTIGATED, AND THEIR DESIGNATIONS

Additive	Designation	Composition of mixture		Additive	Designation	Composition of mixture		
		Weight percent ^a	Equivalent percent ^b			Weight percent ^a	Equivalent percent ^b	
None	0-0	0	0	P mixture	P-1	1.981	0.617	
MgO	M-0.5	0.500	0.308		P-2	3.923	1.238	
	M-1	1.000	.617		P-3	5.827	1.865	
	M-2	2.000	1.238		P-4	7.694	2.496	
	M-3	3.000	1.865		P-6	11.324	3.773	
	M-4	4.000	2.496		P-8	14.819	5.071	
	M-6	6.000	3.773		Q mixture	Q-1	1.656	0.617
	M-8	8.000	5.071			Q-2	3.290	1.238
CeO ₂	C-1	2.110	0.617	Q-3		4.903	1.865	
	C-2	4.174	1.238	Q-4		6.495	2.496	
	C-3	6.192	1.865	Q-6	9.617	3.773		
	C-4	8.167	2.496	Q-8	12.661	5.071		
	C-6	11.990	3.773	R mixture	R-1	1.622	0.617	
	C-8	15.654	5.071		R-2	3.224	1.238	
Y ₂ O ₃	Y-1	1.851	0.617		R-3	4.806	1.865	
	Y-2	3.670	1.238		R-4	6.368	2.496	
	Y-3	5.458	1.865		R-6	9.436	3.773	
	Y-4	7.217	2.496		R-8	12.430	5.071	
	Y-6	10.647	3.773					
	Y-8	13.966	5.071					

^aIn mixture before sintering.

^bAfter sintering, assuming reaction of 0.49 wt. % carbon with SiO₂ to form SiO and CO.

TABLE V. - SHRINKAGE AND WEIGHT LOSSES DURING SINTERING OF Si_3N_4 WITH OXIDE ADDITIVES

Additive	Designation (see table IV)	Sintering temperature, °C									
		1650		1700		1735		1765		1820	
		Shrinkage, percent	Weight loss, percent	Shrinkage, percent	Weight loss, percent	Shrinkage, percent	Weight loss, percent	Shrinkage, percent	Weight loss, percent	Shrinkage, percent	Weight loss, percent
MgO	M-1	9.1	1.2	9.0	2.3	10.3	2.8	9.0	5.7	9.7	10.6
	M-4	12.3	.6	11.8	3.1	12.0	3.8	12.0	10.0	12.0	11.3
	M-8	12.3	.4	10.6	2.2	12.0	4.8	10.1	4.7	10.4	9.3
CeO ₂	C-1	----	---	8.5	0.4	9.6	0	10.3	0.3	11.9	4.2
	C-4	----	---	12.0	1.0	12.2	.4	12.9	1.2	12.6	1.2
	C-8	----	---	11.2	2.2	11.1	.1	11.4	.2	11.7	1.2
Y ₂ O ₃	Y-1	----	---	9.1	1.4	10.0	-0.3	11.5	0.9	13.1	8.9
	Y-4	----	---	10.4	.6	12.1	-.2	12.2	-.3	13.1	1.5
	Y-8	----	---	10.3	-.8	11.9	-1.1	12.4	-.7	12.5	-.6
P mixture	P-1	----	---	8.5	3.1	9.2	0.5	10.1	2.3	11.9	4.2
	P-4	----	---	10.7	.4	12.1	2.2	12.9	.6	12.9	1.7
	P-8	----	---	10.1	.2	11.9	-.3	12.9	.9	12.8	.5
Q mixture	Q-1	----	---	9.7	2.2	9.9	-0.4	11.6	0.7	12.8	8.3
	Q-4	----	---	12.3	1.4	12.0	.5	12.5	.5	12.9	1.3
	Q-8	----	---	11.3	1.0	11.4	.4	12.0	1.2	11.9	1.6
R mixture	R-1	----	---	10.2	2.0	10.5	-0.4	11.6	3.0	12.1	5.1
	R-4	----	---	12.9	.9	12.6	.6	12.7	2.7	12.7	2.6
	R-8	----	---	12.0	.9	10.8	-.1	12.7	1.3	12.5	2.3

TABLE VI. - X-RAY DIFFRACTION ANALYSES OF SINTERED

 Si_3N_4 WITH OXIDE ADDITIVES

Additive	Designation (see table IV)	Sintered at 1765° C ^a	Sintered at 1820° C ^a
MgO	M-4	$\beta\text{-Si}_3\text{N}_4 = \text{vs}$ $\text{Si}_2\text{N}_2\text{O} = \text{vw}$	$\beta\text{-Si}_3\text{N}_4 = \text{vs}$ $\text{Si}_2\text{N}_2\text{O} = \text{vww}$
	M-6	$\beta\text{-Si}_3\text{N}_4 = \text{vs}$ $\text{Si}_2\text{N}_2\text{O} = \text{w}$ Tridymite = m	-----
	M-8	$\beta\text{-Si}_3\text{N}_4 = \text{vs}$	-----
CeO ₂	C-1	$\beta\text{-Si}_3\text{N}_4 = \text{vs}$ $\text{Si}_2\text{N}_2\text{O} = \text{vw}$	-----
	C-4	$\beta\text{-Si}_3\text{N}_4 = \text{vs}$ $\text{Si}_2\text{N}_2\text{O} = \text{vw}$	$\beta\text{-Si}_3\text{N}_4 = \text{vs}$ $\text{Si}_2\text{N}_2\text{O} = \text{w}$ Tridymite = w
	C-8	$\beta\text{-Si}_3\text{N}_4 = \text{vs}$ $\text{Si}_2\text{N}_2\text{O} = \text{vww}$	$\beta\text{-Si}_3\text{N}_4 = \text{vs}$
Y ₂ O ₃	Y-1	$\beta\text{-Si}_3\text{N}_4 = \text{vs}$ $\text{Si}_2\text{N}_2\text{O} = \text{m}$	-----
	Y-2	$\beta\text{-Si}_3\text{N}_4 = \text{vs}$ $\text{Si}_2\text{N}_2\text{O} = \text{m}$	-----
	Y-4	$\beta\text{-Si}_3\text{N}_4 = \text{vs}$ $\text{Si}_2\text{N}_2\text{O} = \text{vww}$	-----
	Y-8	$\beta\text{-Si}_3\text{N}_4 = \text{vs}$	$\beta\text{-Si}_3\text{N}_4 = \text{vs}$
P mixture	P-4	$\beta\text{-Si}_3\text{N}_4 = \text{vs}$ $\text{Si}_2\text{N}_2\text{O} = \text{m}$ Tridymite = s	$\beta\text{-Si}_3\text{N}_4 = \text{vs}$ $\text{Si}_2\text{N}_2\text{O} = \text{vw}$
Q mixture	Q-4	$\beta\text{-Si}_3\text{N}_4 = \text{vs}$ $\text{Si}_2\text{N}_2\text{O} = \text{m}$	$\beta\text{-Si}_3\text{N}_4 = \text{vs}$ $\text{Si}_2\text{N}_2\text{O} = \text{vw}$
R mixture	R-4	$\beta\text{-Si}_3\text{N}_4 = \text{vs}$ $\text{Si}_2\text{N}_2\text{O} = \text{m}$ Si or CeO ₂ = vw $\alpha\text{-Cristobalite} = \text{vww}$	$\beta\text{-Si}_3\text{N}_4 = \text{vs}$ $\text{Si}_2\text{N}_2\text{O} = \text{vw}$

^am = medium; s = strong; w = weak; vs = very strong; vw = very weak; vww = very, very weak.

1. Report No. NASA TP-1644	2. Government Accession No.	3. Recipient's Catalog No.	
4. Title and Subtitle EFFECT OF OXIDE ADDITIONS AND TEMPERATURE ON SINTERABILITY OF MILLED SILICON NITRIDE		5. Report Date April 1980	6. Performing Organization Code
		8. Performing Organization Report No. E-243	10. Work Unit No. 505-01
7. Author(s) Alan Arias		11. Contract or Grant No.	
9. Performing Organization Name and Address National Aeronautics and Space Administration Lewis Research Center Cleveland, Ohio 44135		13. Type of Report and Period Covered Technical Paper	
		14. Sponsoring Agency Code	
12. Sponsoring Agency Name and Address National Aeronautics and Space Administration Washington, D.C. 20546		15. Supplementary Notes	
16. Abstract Specimens of milled α - Si_3N_4 with 0 to 5.07 equivalent percent of oxide additions were pressureless sintered at 1650 ^o to 1820 ^o C for 4 hours in nitrogen while covered with powdered Si_3N_4 + SiO_2 . Densities \geq 97.5 percent of theoretical resulted with \sim 2.5 equivalent percent of MgO , CeO_2 , Y_2O_3 , and three mixtures involving these oxides. Densities \geq 94 percent of theoretical were obtained with \sim 0.62 equivalent percent of the same additives. At most temperatures, best sinterability (density maxima) was obtained with \sim 1.2 to 2.5 equivalent percent additive.			
17. Key Words (Suggested by Author(s)) Ceramics Silicon nitride Sintering		18. Distribution Statement Unclassified - unlimited STAR Category 27	
19. Security Classif. (of this report) Unclassified	20. Security Classif. (of this page) Unclassified	21. No. of Pages 20	22. Price* A02

* For sale by the National Technical Information Service, Springfield, Virginia 22161.

NASA-Langley, 1980